Modeling and analysis of $N_2(B^3\Pi_g)$ and $N_2(C^3\Pi_u)$ vibrational distributions in sprites

A. Luque[1] and F. J. Gordillo-Vázquez[1]

Received 20 July 2010; revised 25 November 2010; accepted 15 December 2010; published 8 February 2011.

[1] We analyze and model available data of $N_2(B^3\Pi_g)$ vibrational distribution functions (VDF) in sprites, and we present model predictions for the VDF of $N_2(C^3\Pi_u)$. By means of a full kinetic model and a simplified steady state model presented here, we investigate sprites at altitudes of 52 km up to 85 km, observed with temporal resolutions from 33 ms to 50 μs. At all altitudes, the predictions of the models agree with available observations of the VDF of $N_2(B^3\Pi_g)$. We find that the VDF of $N_2(B^3\Pi_g)$ and $N_2(C^3\Pi_u)$ depend very weakly on the driving electric field. In addition, we find that while the $N_2(B^3\Pi_g)$ VDF is barely affected by changes in the temporal resolution, the VDF of $N_2(C^3\Pi_u)$ is not affected at all.

Citation: Luque, A., and F. J. Gordillo-Vázquez (2011), Modeling and analysis of $N_2(B^3\Pi_g)$ and $N_2(C^3\Pi_u)$ vibrational distributions in sprites, *J. Geophys. Res.*, *116*, A02306, doi:10.1029/2010JA015952.

1. Introduction

[2] Spectral studies of sprites started in the mid 1990s with the simultaneous works by *Mende et al.* [1995] and *Hampton et al.* [1996]. These two groups independently reported spectra of the red emission from the N_2 first positive system in the spectral range between 450 nm and 800 nm (840 nm in the case of *Hampton et al.* [1996]) and with original spectral resolutions of 6 nm and 10 nm [*Hampton et al.*, 1996] and 9 nm [*Mende et al.*, 1995]. Both groups recorded the spectra with a temporal resolution of 33 ms. However, the spectrograph slit of *Mende et al.* [1995] was vertically oriented while in the case of *Hampton et al.* [1996] it was parallel to the horizon. Consequently, the spectrum obtained by *Mende et al.* [1995] contains emission from a range of altitudes between 74 km and 90 km, while the spectrum by *Hampton et al.* [1996] corresponds to sprite emissions at around 70 km altitude. *Green et al.* [1996] was the first to discuss the nature of the molecular excitation processes underlying visible light emission from sprites and to provide a preliminary quantitative analysis of the relative populations of the vibrational levels in $N_2(B^3\Pi_g, v)$ up to $v = 10$, derived from the measurements reported by *Mende et al.* [1995] and *Hampton et al.* [1996]. *Morrill et al.* [1998] extended the observed sprite spectral range into the very near infrared (900 nm), estimating for the first time the relative population of the $v = 1$ vibrational level of $N_2(B^3\Pi_g)$ at low altitude (53–57 km). Later *Bucsela et al.* [2003] analyzed sprite spectra from the tendril region of sprites from observations previously reported by *Morrill et al.* [1998]. They discussed measurements from two different spectrographs, both with horizontal slits but with different spectral resolutions (0.7 nm for 53 km and 1.1 nm for 57 km). The results by *Bucsela et al.* [2003] included error bars and showed a different behavior for the VDF of $N_2(B^3\Pi_g)$ at 53 km and 57 km, with an enhancement at $v = 2$ for an altitude of 57 km. As acknowledged by the authors, this was probably an effect of sensitivity calibration errors. Recent observations by *Kanmae et al.* [2007] with improved spectral (3 nm) and temporal resolution (3 ms) exhibit an altitude variation of the vibrational populations within the $B^3\Pi_g$ state of N_2. At low altitude the populations in the higher levels fall off more rapidly relative to the population with $v = 2$.

[3] *Gordillo-Vázquez* [2010] presented the first full kinetic model to include detailed vibrational kinetics of sprites. The prediction of this model at 78 km agreed with the VDF of $N_2(B^3\Pi_g)$ in the 84.4–86.4 km range measured by *Kanmae et al.* [2007]. Besides, the model of *Gordillo-Vázquez* [2010] predicted the shape and trend of the VDF of $N_2(C^3\Pi_u)$ at 78 km for different temporal resolutions.

[4] Very recently *Kanmae et al.* [2010b] measured spectra of sprite streamer heads using, for the first time, slitless spectroscopy with a recording rate of 10000 fps (0.1 ms temporal resolution). These authors estimated the VDF of $N_2(B^3\Pi_g)$, between $v = 2$ and $v = 5$, at about 62 km altitude and compared it with predictions of a simplified kinetic model that includes two possible sets of quenching rates for $N_2(B^3\Pi_g, v)$. The modeled VDF (normalized to $v = 2$) of *Kanmae et al.* [2010b] only shows good agreement for $v = 4$. According to the authors, the large discrepancy at $v = 3$ resulted from an inaccurate determination of the observed spectrum. Subsequent work by the same group [*Kanmae et al.*, 2010a] applies the same spectroscopic technique to blue sprite emissions.

[5] Finally, we note that *Heavner et al.* [2010] has recently reported near-ultraviolet (NUV) and blue (320–

[1]IAA-CSIC, Granada, Spain.

0148-0227/11/2010JA015952

460 nm) spectra of sprites at 65 km altitude, focusing on emissions from $N_2(C^3\Pi_u)$. These observations were carried out during the EXL98 aircraft sprite observation campaign in July 1998, using a NUV horizontal spectrograph slit with 4 nm spectral resolution and 60 fps recording rate. This paper shows a NUV spectrum and the authors claim to have determined the VDF of $N_2(C^3\Pi_u)$ which is, however, not shown in the paper.

[6] Here we use the detailed sprite atmospheric kinetic model of *Gordillo-Vázquez* [2008], *Gordillo-Vázquez and Donkó* [2009], and *Gordillo-Vázquez* [2010] together with a simplified steady state vibrational kinetic model recently developed. We analyze the available data for the VDF of $N_2(B^3\Pi_g)$ and predict the VDF of $N_2(C^3\Pi_u)$ in sprites at several altitudes and observed with different temporal resolutions.

2. Analysis

2.1. Data

[7] Our analysis is mostly based on VDF data by *Bucsela et al.* [2003] (partly based on previous results by *Morrill et al.* [1998]) for 53 km and 57 km and by *Kanmae et al.* [2007] for altitudes ranging from 55 km to 85 km. The latter sets measured the VDF of $N_2(B^3\Pi_g)$ and includes an estimation of errors, absent in older VDF data by *Mende et al.* [1995] and *Hampton et al.* [1996].

[8] In the literature the VDF is often normalized by dividing by the population of the lowest accessible vibrational level, in many cases $v = 2$. However, given the limited wavelength window of most sprite spectrographs, the information about the $v = 2$ state is usually extracted from the single decay of this state toward $v = 0$ of $N_2(A^3\Sigma_u^+)$ [*Kanmae et al.*, 2007], whereas for higher v in $N_2(B^3\Pi_g)$ one can observe two and up to three vibrational transitions. Hence the state $v = 2$ of $N_2(B^3\Pi_g)$ has a higher uncertainty which is propagated to other states in the normalization.

[9] We chose instead to include in the normalization all vibrational states available in the observations under analysis, namely from $v = 2$ to $v = 6$ and from $v = 0$ to $v = 4$ for $N_2(B^3\Pi_g)$ and $N_2(C^3\Pi_u)$, respectively.

2.2. Full Kinetic Model

[10] The full sprite atmospheric kinetic model used in this paper is described in detail by *Gordillo-Vázquez* [2008, 2010]. This models builds on previous studies on the vibrational and electronic kinetics of air plasmas both at high altitudes, such as those by *Cartwright* [1978] and *Morrill et al.* [1998], and in the laboratory, such as those by *Cacciatore et al.* [1982] and *Capitelli et al.* [1986]. It assumes that most of the chemical activity of sprites begins in their brightest regions, that is, in their initial and very short living streamer heads [*Sentman et al.*, 2008b, 2008a]. The duration of the sprite streamer heads have not yet been completely resolved in time but recent high-speed sprite imaging at 10000 frames per second (with 50 μs exposure time) [*McHarg et al.*, 2007; *Stenbaek-Nielsen et al.*, 2007] shows the expected point-like structure of the streamer heads. Therefore, the full sprite atmospheric kinetic model used here considers sprites as impulsive discharges in air with a pulse duration of 5 μs.

[11] The present sprite, full kinetic, atmospheric model solves the coupled Boltzmann transport equation (to derive the electron energy distribution function (EEDF)) with the rate equations associated to each of the different species considered (electrons, ions, atoms and molecules) and each of the electronically and vibrationally excited species. For N_2 we included the states $N_2(X^1\Sigma_2^+, v = 0–8)$, $N_2(A^3\Sigma_u^+, v = 0–16)$, $N_2(B^3\Pi_g, v = 0–6)$, $N_2(C^3\Pi_u, v = 0–4)$, $N_2(a^1\Pi_g, v = 0–15)$, $N_2(a'^1\Sigma_u^-)$, $N_2(w^1\Delta_u, v = 0–3)$ and $N_2(B'^3\Sigma_u^-, v = 0–1)$; for O_2 we considered $O_2(X^3\Sigma_g^-)$, $O_2(a'\Delta_g)$ and $O_2(b'\Sigma_g^+)$. In this way, all the kinetics are self-consistent, although, in the present approach, the electrodynamics is not consistently solved with the plasma kinetics since the Poisson equation is not considered. In this regard, it has been assumed that the reduced electric field (E/N, where N is the gas density at a given altitude), within the streamer head plasma is an external parameter of the model and that it exhibits a step-like shape. We used $E/N = 250$ Townsend (Td) and 400 Td (at 55 km altitude), 425 Td and 700 Td (at 74 km altitude) and 500 Td and 900 Td (at 85 km altitude). The Townsend is the conventional unit for reduced electric fields, $1\ \text{Td} = 10^{-17}\ \text{V cm}^2$. These values are assumed during a short time interval of 5 μs while, afterward, $E/N = 30$ Td. The low field value after the pulse is characteristic of the region behind sprite streamer heads [*McHarg et al.*, 2007; *Luque and Ebert*, 2010; *Gordillo-Vázquez and Luque*, 2010]; there the electron-driven kinetics becomes of secondary importance compared to the processes controlled by the collisions between ground and excited heavy species.

[12] However, some changes have been now included in that model. As discussed below, we have replaced the rates of quenching of $N_2(B^3\Pi_g)$ by N_2 and O_2. The old set of parameters, used by *Gordillo-Vázquez* [2010] and the new set, used here, are described in section 2.4, where we also discuss the rationale behind this update.

2.3. Simplified Steady State Kinetic Model

[13] As a complement to the full kinetic model, we present here a "minimal" model that, containing as few elements and assumptions as possible, can accurately describe the observed VDF of $N_2(B^3\Pi_g)$ in sprites.

[14] We consider the vibrational populations of the electronic states $N_2(B^3\Pi_g)$ and $N_2(C^3\Pi_u)$, which are produced by electron impact excitation of the fundamental state $N_2(X^1\Sigma_g^+)$. We also take into account collisional quenching with $N_2(X^1\Sigma_g^+)$ and radiative transitions $N_2(B^3\Pi_g) \rightarrow N_2(A^3\Sigma_u^+)$ and $N_2(C^3\Pi_u) \rightarrow N_2(B^3\Pi_g)$. At a given location $\mathbf{x}$, the time variation of the population for each of the electronic levels reads

$$\frac{dC_v(\mathbf{x},t)}{dt} = F_v^C \nu_C(\mathbf{x},t) n_e(\mathbf{x},t) - \left[\sum_{v'} A_{vv'}^{C\rightarrow B}\right] C_v(\mathbf{x},t) - q_v^C N(\mathbf{x}) C_v(\mathbf{x},t), \tag{1a}$$

$$\frac{dB_v(\mathbf{x},t)}{dt} = F_v^B \nu_B(\mathbf{x},t) n_e(\mathbf{x},t) - \left[\sum_{v'} A_{vv'}^{B\rightarrow A}\right] B_v(\mathbf{x},t) - q_v^B N(\mathbf{x}) B_v(\mathbf{x},t) + \sum_{v'} A_{v'v}^{C\rightarrow B} C_{v'}(\mathbf{x},t), \tag{1b}$$

where $N(\mathbf{x})$ is the air density at $\mathbf{x}$ and $B_v(\mathbf{x}, t) = [N_2(B^3\Pi_g, v)]$, $C_v(\mathbf{x}, t) = [N_2(C^3\Pi_u, v)]$. For each electronic level $Y = B$ or $Y = C$, F_v^Y, are the Franck-Condon factors and $\nu_Y(\mathbf{x}, t)$ is the rate of electron impact excitation per electron and unit time ($\nu_Y(\mathbf{x}, t) = [N_2]k_Y(\mathbf{x}, t)$, with k_Y the chemical reaction rate), $A_{vv'}^{Y\to Z}$ is the Einstein coefficient for a spontaneous radiative transition between electronic states Y and Z and vibrational levels v, v' and q_v^Y is the combined quenching rate due to collisions with ground state N_2 and O_2 (which we assume are mixed in a 80:20 ratio). Finally, $n_e(\mathbf{x}, t)$ is the electron density. In our calculations we used the Franck-Condon factors and the Einstein coefficients tabulated by *Gilmore et al.* [1992]; the quenching rates are discussed below.

[15] Now let us assume that a spectrograph is observing a volume V inside the sprite discharge and assume that the vertical extent of V is small enough that the density of air, $N(\mathbf{x})$ can be regarded as constant (that is, we are observing only close to a given altitude). We also assume that an observation from the spectrograph integrates all emissions from V during a time interval $(0, T)$. To calculate the emissions recorded by the spectrograph we integrate (1) in the volume V and in the interval T. The left hand side of (1a) gives $\int_V C_v(\mathbf{x}, T)d^3\mathbf{x} - \int_V C_v(\mathbf{x}, 0)d^3\mathbf{x}$. This vanishes if either of the following conditions hold: (a) V is large enough that it contains many emitters, each at a different stage of the excitation-emission process, so the integrated populations of $N_2(C^3\Pi_u, v)$ do not change during T (that is, we are looking at a spatially averaged steady state inside V) or (b) T is long enough that the full excitation-radiation process occurs during the integration time. In most cases either condition a or condition b holds at least approximately and the same argument can be applied to (1b) so after the integration we can neglect the left hand sides of (1) and we arrive at

$$0 = F_v^C\overline{f_C} - K_v^C\overline{C}_v, \tag{2a}$$

$$0 = F_v^B\overline{f_B} - K_v^B\overline{B}_v + \sum_{v'} A_{v'v}^{C\to B}\overline{C}_{v'}, \tag{2b}$$

where to simplify the notation we introduced

$$K_v^C = \sum_{v'} A_{vv'}^{C\to B} + q_v^C N,$$

$$K_v^B = \sum_{v'} A_{vv'}^{B\to A} + q_v^B N,$$

$$f_C(t) = \nu_C(t)n_e(t),$$

$$f_B(t) = \nu_B(t)n_e(t),$$

and a bar over a variable is a shortcut to denote integration in volume and time, $\overline{X} = \int_V\int_0^T X(\mathbf{x}, t)\, dt\, d^3\mathbf{x}$.

[16] The system (2) is a linear system of equations that can be solved for the integrated populations $\overline{B}_v$ and $\overline{C}_v$. However, since absolute radiances are often not accessible experimentally we are interested not in the populations of each vibrational level but in the normalized VDF, defined as

$$b_v = \frac{\overline{B}_v}{\sum_{v'}\overline{B}_{v'}}, \tag{3a}$$

$$c_v = \frac{\overline{C}_v}{\sum_{v'}\overline{C}_{v'}}. \tag{3b}$$

In this model the VDF of $N_2(C^3\Pi_u)$ is completely determined by (2a) as

$$c_v = \frac{F_v^C/K_v^C}{\sum_v F_v^C/K_v^C}, \tag{4}$$

depending only on tabulated parameters. But the VDF of $N_2(B^3\Pi_g)$, after manipulations, can be expressed as

$$b_v = \frac{(1-w)N_0(v) + wN_1(v)}{(1-w)Z_0 + wZ_1}, \tag{5}$$

where

$$N_0(v) = F_v^B/K_v^B, \quad Z_0 = \sum_v N_0(v), \tag{6a}$$

$$N_1(v) = \frac{1}{K_v^B}\sum_{v'}\frac{A_{v'v}^{C\to B}F_{v'}^C}{K_{v'}^C}, \quad Z_1 = \sum_v N_1(v), \tag{6b}$$

and

$$w = \frac{\overline{f_C}}{\overline{f_B} + \overline{f_C}}. \tag{7}$$

[17] Note that the values defined in (6) depend only on tabulated parameters and the density of air (in the auxiliary material we give computer-readable tables with the values of $N_0(v)$, $N_1(v)$, Z_0 and Z_1 at several altitudes derived from two alternative sets of quenching rates).[1] Therefore at a given pressure, (5) expresses the VDF of $N_2(B^3\Pi_g)$ as a function of the single parameter w, as a formal combination of two limiting VDFs, corresponding to $w = 0$ and $w = 1$. The physical interpretation of w is clear: it is the ratio of the total number of electron impact excitations of the $N_2(C^3\Pi_u)$ level to the combined number of electron impact excitations of both $N_2(B^3\Pi_g)$ and $N_2(C^3\Pi_u)$. In the limit $w = 0$ there are only excitations of the $N_2(B^3\Pi_g)$ level, which has a lower threshold energy, and $b_v = N_0(v)/Z_0$; this corresponds to low electric fields. When w is high, excitations of the $N_2(C^3\Pi_u)$ state, which has a higher energy threshold, dominate; in this case the $N_2(B^3\Pi_g)$ state is populated mostly by radiative cascading from $N_2(C^3\Pi_u)$. Since even at very high reduced

[1] Auxiliary materials are available at ftp://ftp.agu.org/apend/ja/2010JA015952.

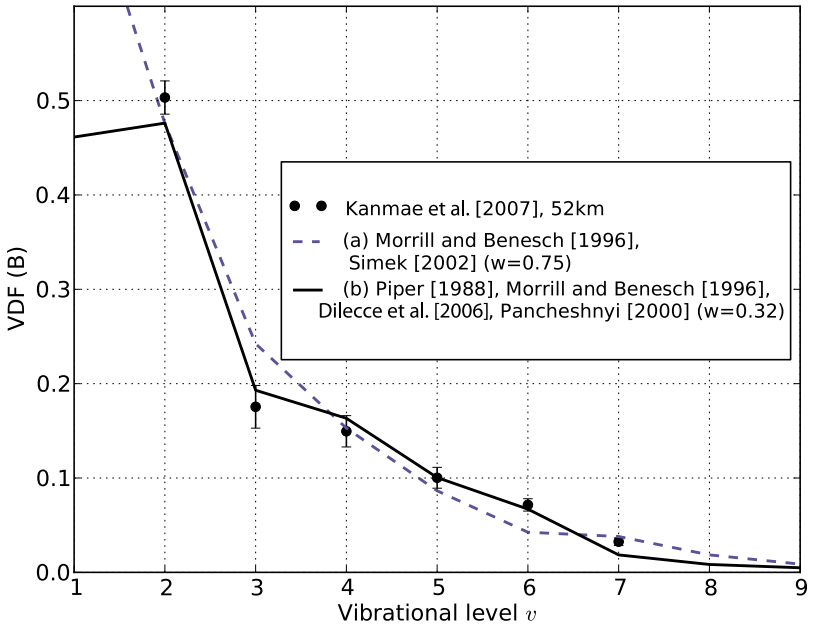

Figure 1. Observation of the VDF for the $N_2(B^3\Pi_g)$ at 55 km [*Kanmae et al.*, 2007] and comparison with the best fits from the steady state model using the quenching rates from (a) the parameters used by *Gordillo-Vázquez* [2010], i.e., those of *Morrill and Benesch* [1996] for quenching of $N_2(B^3\Pi_g)$ by O_2 and N_2 and *Simek* [2002] for quenching of $N_2(C^3\Pi_u)$ by N_2 (quenching of $N_2(C^3\Pi_u)$ by O_2 is neglected), and (b) an improved set of parameters with the rates from *Piper* [1988] for quenching of $N_2(B^3\Pi_g)$ by N_2, *Morrill and Benesch* [1996] for quenching of $N_2(B^3\Pi_g)$ by O_2, *Dilecce et al.* [2006] for quenching of $N_2(C^3\Pi_u)$ by N_2, and *Pancheshnyi* [2000] for quenching of $N_2(C^3\Pi_u)$ by O_2.

electric fields there is a nonnegligible excitation of the $N_2(B^3\Pi_g)$ state the limiting value $w = 1$ is never physically attained; we estimate the highest value of w as $w_{max} \approx 0.73$. We note that the parameter w is a functional of the complete temporal and spatial dependence of the electron density and the electron impact excitation rate; establishing a precise relation between w and the reduced electric fields inside the sprite is possible only with additional assumptions and models that are outside the scope of this article.

[18] The advantage of this reduced model is that the full VDF of the $N_2(B^3\Pi_g)$ belongs to a single-parameter family of VDF, making it easy to fit w to any observed VDF. As we will see below, the model fits reasonably well VDFs reported in the previous literature.

2.4. Quenching Rates

[19] The quenching of the excited $N_2(B^3\Pi_g)$ and $N_2(C^3\Pi_u)$ states by collisions with N_2 and O_2 molecules in their ground states significantly affects the VDF, particularly at low altitudes (e.g., 55 km). *Kanmae et al.* [2010b] used two sets of quenching rates to analyze their observations: those detailed by *Piper* [1988] and those provided by *Morrill and Benesch* [1996]. The latter set was also used in our original kinetic model [*Gordillo-Vázquez*, 2010].

[20] The steady state model described above provides an additional tool to evaluate these quenching rates. The reason is that the temporal and spatial dependence of the electric fields in the emitting region is abstracted away by the single parameter w. Therefore a least squares fit of w to the observational data shows, for each set of quenching rates and without any additional assumption, the best possible agreement between the model and the observation.

[21] In Figure 1 we show the best fits to the VDF of $N_2(B^3\Pi_g)$ observed by *Kanmae et al.* [2007]. We compare two sets: the first one (set a) represents the parameters used by *Gordillo-Vázquez* [2010], based on work by *Morrill and Benesch* [1996] for quenching of $N_2(B^3\Pi_g)$ by O_2 and N_2 and *Simek* [2002] for quenching of $N_2(C^3\Pi_u)$ by N_2, (quenching of $N_2(C^3\Pi_u)$ by O_2 is neglected). The second set (set b) is the one used here; it incorporates rates from *Piper* [1988] for quenching of $N_2(B^3\Pi_g)$ by N_2, *Morrill and Benesch* [1996] for quenching of $N_2(B^3\Pi_g)$ by O_2, *Dilecce et al.* [2006] for quenching of $N_2(C^3\Pi_u)$ by N_2 and *Pancheshnyi* [2000] for quenching of $N_2(C^3\Pi_u)$ by O_2.

[22] The second set is much closer to the observations; in particular, it exhibits a large ratio between the population of $N_2(B^3\Pi_g, v = 2)$ and $N_2(B^3\Pi_g, v = 3)$, similar to the observed VDF. This is the reason that we have opted to use the quenching rates of set b, both in the full kinetic model and in the steady state model.

3. Results and Discussion

[23] The VDFs for $N_2(B^3\Pi_g)$ and $N_2(C^3\Pi_u)$ are shown in Figure 2 (top) and Figure 2 (bottom), respectively.

[24] For $N_2(B^3\Pi_g)$, we show the data from *Kanmae et al.* [2007] at the three altitudes that they studied, as well as the observations of *Bucsela et al.* [2003] that we consider close

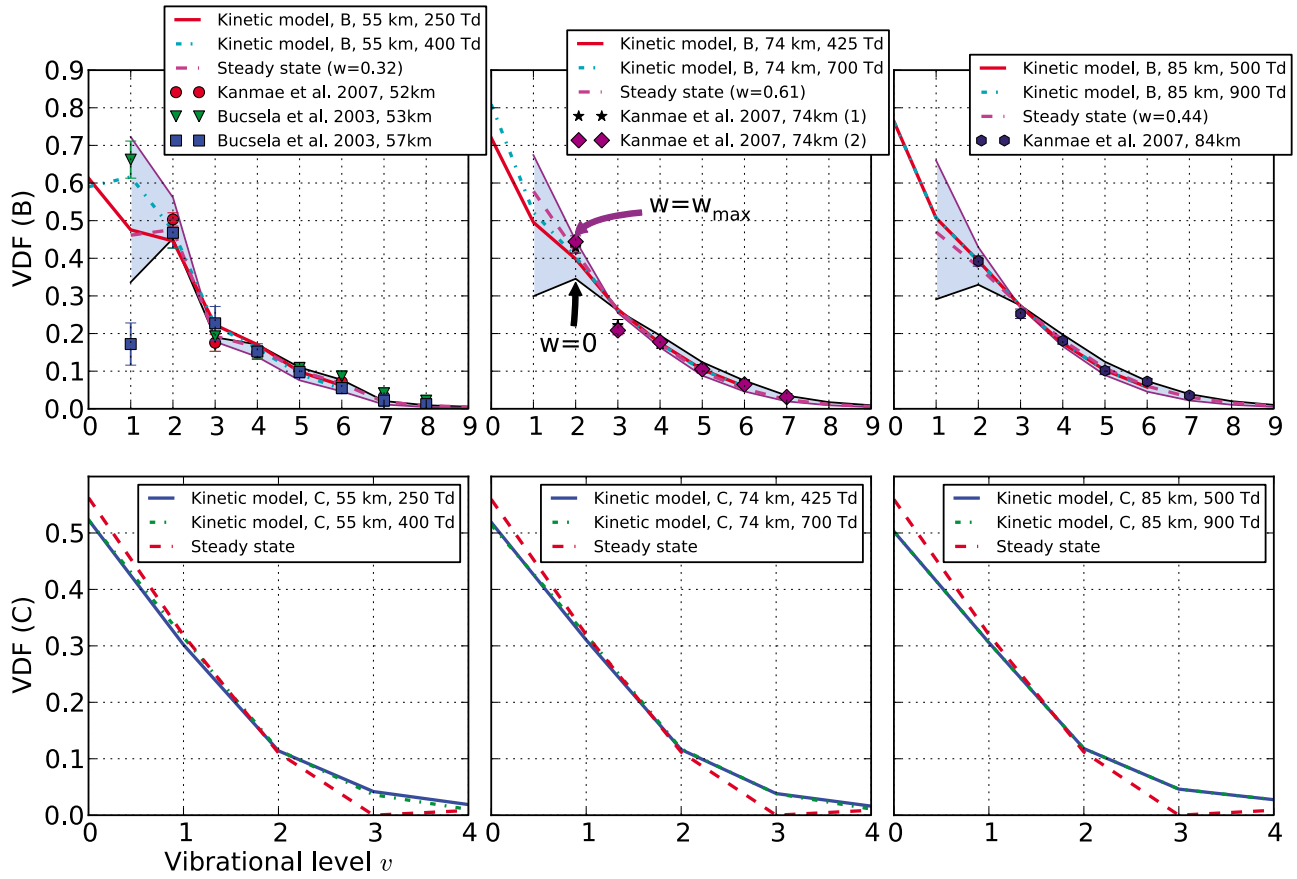

Figure 2. Vibrational distribution function (VDF) for the (top) $N_2(B^3\Pi_g)$ and (bottom) $N_2(C^3\Pi_u)$ electronic states of N_2 at different altitudes. The shaded areas represent the range of variation of the simplified model between the two extremes $w = 0$ (low fields) and $w = w_{max}$ (high fields). In the full kinetic model we used a temporal resolution of 3 ms. The observations by *Kanmae et al.* [2007] were performed also with 3 ms time resolution, whereas in work by *Bucsela et al.* [2003] it was 17 ms.

to the 52–55 km range analyzed by *Kanmae et al.* [2007]. At each altitude we also show the prediction of the full kinetic model with two sample electric fields corresponding to lower and upper limits of reduced electric fields at those altitudes for which predictions of the full kinetic model for the electron density in streamer heads agree with sprite streamer modeling [*Luque and Ebert*, 2009, 2010]. Finally we use the simplified, steady state model to fit w with least squares to the values of *Kanmae et al.* [2007]. The shaded area represents the predicted range of variation in the $N_2(B^3\Pi_g)$ VDF between $w = 0$ (low field) and $w = w_{max}$ (high field) according to the simplified steady state model.

[25] In Figure 2 (bottom) we provide model predictions for the VDF of the $N_2(C^3\Pi_u)$ state, both using the full kinetic model and the simplified model (4) which in this case is parameter free.

[26] First, we notice that both the full model and steady state model exhibit quite fair agreement with available observations at low altitudes where vibrational quenching of $N_2(B^3\Pi_g)$ by N_2 plays a distinct role. At higher altitudes of 74 km and 85 km, model agreement with *Kanmae et al.* [2007] data remains good.

[27] However, we also notice that different values of the input reduced electric field for the full kinetic model provide almost the same good agreement to the observations for $v \geq 2$. Similarly, the steady state simplified model predicts a very narrow range of variation between the low and high field cases. Unfortunately, this field insensibility of the VDF implies that, besides the validation of model parameters, little information can be obtained about the discharge field if only the states with $v \geq 2$ are accessible. In this case, measuring the ratio of the second positive emissions of neutral N_2 to first negative emissions of ionized N_2^+ is probably a more accurate procedure to estimate reduced electric fields in sprites [*Morrill et al.*, 2002; *Celestin and Pasko*, 2010].

[28] As seen from Figure 2, the relative population of the state $N_2(B^3\Pi_g, v = 1)$ is clearly more sensitive to the electric field. But the available experimental value for this population has a considerable uncertainty as indicated by the difference between values reported at 53 km and 57 km [*Bucsela et al.*, 2003]. In this regard, near-infrared (NIR) optical observations of sprites such as those recently reported by *Siefring et al.* [2010] would be very useful. NIR sprite spectra in the 900 nm to 2 μm spectral range can access vibrational transitions of the first positive system (1 PG) of N_2 involving $v = 1$ and $v = 0$. This would give experimental access to the range of the $N_2(B^3\Pi_g)$ VDF that is more sensitive to electric field variations.

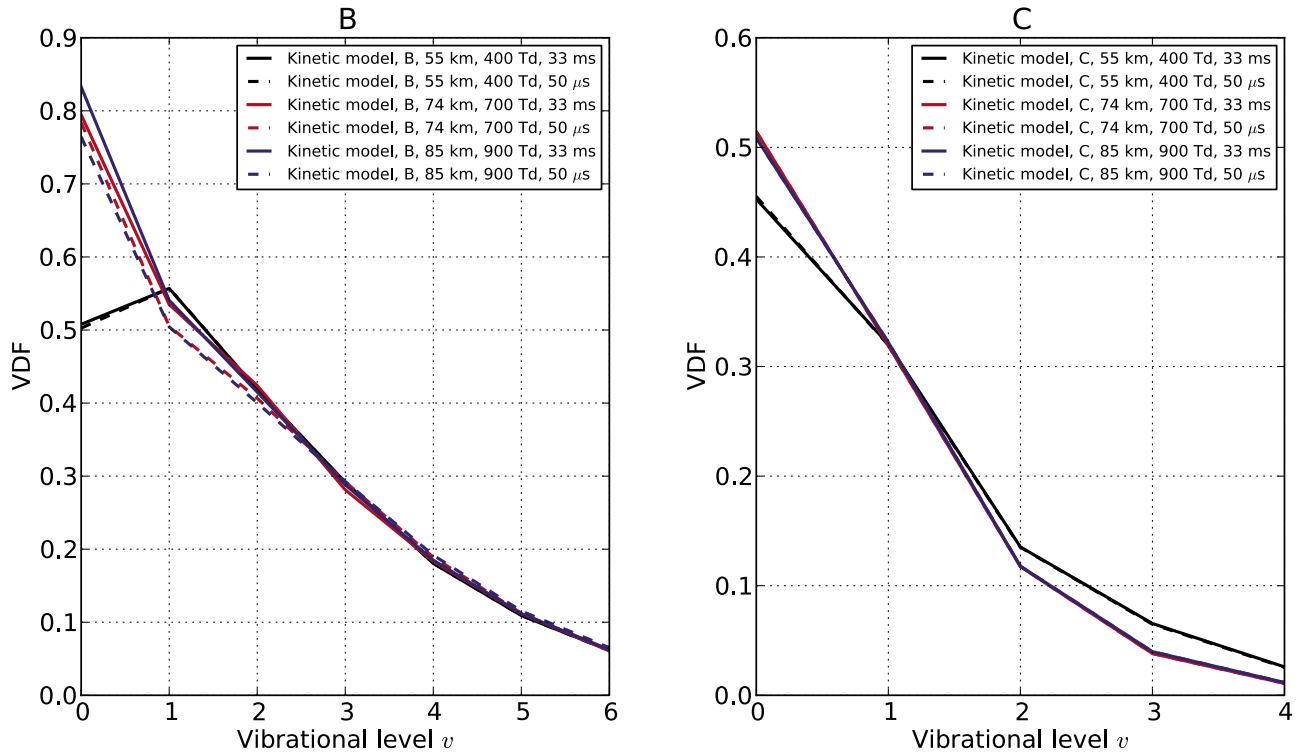

Figure 3. The influence of the temporal resolution of the spectrometer on the observed VDF, according to our full kinetic model. As representative cases, at each altitude we used the highest field represented in Figure 2, and we plot the differences between a gate time of 33 ms (as *Mende et al.* [1995] and *Hampton et al.* [1996]) and 50 μs (as *Kanmae et al.* [2010b]).

[29] A final question that we have addressed with the full kinetic model (but not with the steady state one) is the relevance of the temporal resolution of the spectrograph on the VDF. As Figure 3 shows, the dependence of the VDF on this parameter is very small for the $N_2(B^3\Pi_g)$ state and negligible for the $N_2(C^3\Pi_u)$ state. Consequently, sprite spectroscopy performed with low (33 ms) or very high (0.05 ms) time resolution would produce very similar VDFs.

[30] **Acknowledgments.** We thank M. Simek for helpful discussions about this work. This work was supported by the Spanish Ministry of Science and Innovation, MICINN, under project AYA2009-14027-C05-02.

[31] Robert Lysak thanks the reviewers for their assistance in evaluating this paper.

References

Bucsela, E., J. Morrill, M. Heavner, C. Siefring, S. Berg, D. Hampton, D. Moudry, E. Wescott, and D. Sentman (2003), $N_2(B^3\Pi_g)$ and $N_2^+(A^2\Pi_u)$ vibrational distributions observed in sprites, *J. Atmos. Sol. Terr. Phys.*, *65*, 583–590, doi:10.1016/S1364-6826(02)00316-4.

Cacciatore, M., M. Capitelli, C. Grose, R. Massabieaux, and A. Ricard (1982), The influence of ground-state vibrationally excited N_2 molecules on the vibrational excitation of N_2, N_2^+ electronic states, *Lett. Nuovo Cimento Soc. Ital. Fis.*, *34*, 417–423, doi:10.1007/BF02754798.

Capitelli, M., C. Gorse, and A. Ricard (1986), Coupling of vibrational and electronic energy distributions in discharge and post-discharge conditions, in *Nonequilibrium Vibrational Kinetics*, edited by M. Capitelli, pp. 315–338, Springer, New York.

Cartwright, D. C. (1978), Vibrational populations of the excited states of N_2 under auroral conditions, *J. Geophys. Res.*, *83*, 517–531, doi:10.1029/JA083iA02p00517.

Celestin, S., and V. P. Pasko (2010), Effects of spatial non-uniformity of streamer discharges on spectroscopic diagnostics of peak electric fields in transient luminous events, *Geophys. Res. Lett.*, *37*, L07804, doi:10.1029/2010GL042675.

Dilecce, G., P. F. Ambrico, and S. De Benedictis (2006), OODR-LIF direct measurement of $N_2(C^3\Pi_u, v = 0–4)$ electronic quenching and vibrational relaxation rate coefficients by N_2 collision, *Chem. Phys. Lett.*, *431*, 241–246, doi:10.1016/j.cplett.2006.09.094.

Gilmore, F. R., R. R. Laher, and P. J. Espy (1992), Franck-Condon factors, r-centroids, electronic transition moments, and Einstein coefficients for many nitrogen and oxygen band systems, *J. Phys. Chem. Ref. Data*, *21*, 1005–1107.

Gordillo-Vázquez, F. J. (2008), Air plasma kinetics under the influence of sprites, *J. Phys. D Appl. Phys.*, *41*(23), 234016, doi:10.1088/0022-3727/41/23/234016.

Gordillo-Vázquez, F. J. (2010), Vibrational kinetics of air plasmas induced by sprites, *J. Geophys. Res.*, *115*, A00E25, doi:10.1029/2009JA014688.

Gordillo-Vázquez, F. J., and Z. Donkó (2009), Electron energy distribution functions and transport coefficients relevant for air plasmas in the troposphere: Impact of humidity and gas temperature, *Plasma Sources Sci. Technol.*, *18*(3), 034021, doi:10.1088/0963-0252/18/3/034021.

Gordillo-Vázquez, F. J., and A. Luque (2010), Electrical conductivity in sprite streamer channels, *Geophys. Res. Lett.*, *37*, L16809, doi:10.1029/2010GL044349.

Green, B. D., et al. (1996), Molecular excitation in sprites, *Geophys. Res. Lett.*, *23*, 2161–2164, doi:10.1029/96GL02071.

Hampton, D. L., M. J. Heavner, E. M. Wescott, and D. D. Sentman (1996), Optical spectral characteristics of sprites, *Geophys. Res. Lett.*, *23*, 89–92, doi:10.1029/95GL03587.

Heavner, M. J., J. S. Morrill, C. L. Siefring, D. Sentman, D. Moudrey, E. Wescott, and E. Bucsela (2010), Near-ultraviolet and blue spectral observations of sprites in the 320–460 nm region: N_2(2PG) emissions, *J. Geophys. Res.*, *115*, A00E44, doi:10.1029/2009JA014858.

Kanmae, T., H. C. Stenbaek-Nielsen, and M. G. McHarg (2007), Altitude resolved sprite spectra with 3 ms temporal resolution, *Geophys. Res. Lett.*, *34*, L07810, doi:10.1029/2006GL028608.

Kanmae, T., H. Stenbaek-Nielsen, M. G. McHarg, and R. K. Haaland (2010a), Observation of blue sprite spectra at 10,000 fps, *Geophys. Res. Lett.*, *37*, L13808, doi:10.1029/2010GL043739.

Kanmae, T., H. Stenbaek-Nielsen, M. G. McHarg, and R. K. Haaland (2010b), Observation of sprite streamer head's spectra at 10,000 fps, *J. Geophys. Res.*, *115*, A00E48, doi:10.1029/2009JA014546.

Luque, A., and U. Ebert (2009), Emergence of sprite streamers from screening-ionization waves in the lower ionosphere, *Nat. Geosci.*, *2*, 757–760, doi:10.1038/ngeo662.

Luque, A., and U. Ebert (2010), Sprites in varying air density: Charge conservation, glowing negative trails and changing velocity, *Geophys. Res. Lett.*, *37*, L06806, doi:10.1029/2009GL041982.

McHarg, M. G., H. C. Stenbaek-Nielsen, and T. Kammae (2007), Observations of streamer formation in sprites, *Geophys. Res. Lett.*, *34*, L06804, doi:10.1029/2006GL027854.

Mende, S. B., R. L. Rairden, G. R. Swenson, and W. A. Lyons (1995), Sprite spectra; N_2 1 PG band identification, *Geophys. Res. Lett.*, *22*, 2633–2636, doi:10.1029/95GL02827.

Morrill, J. S., and W. M. Benesch (1996), Auroral N_2 emissions and the effect of collisional processes on N_2 triplet state vibrational populations, *J. Geophys. Res.*, *101*, 261–274, doi:10.1029/95JA02835.

Morrill, J. S., E. J. Bucsela, V. P. Pasko, S. L. Berg, M. J. Heavner, D. R. Moudry, W. M. Benesch, E. M. Wescott, and D. D. Sentman (1998), Time resolved N2 triplet state vibrational populations and emissions associated with red sprites, *J. Atmos. Sol. Terr. Phys.*, *60*, 811–829, doi:10.1016/S1364-6826(98)00031-5.

Morrill, J., et al. (2002), Electron energy and electric field estimates in sprites derived from ionized and neutral N_2 emissions, *Geophys. Res. Lett.*, *29*(10), 1462, doi:10.1029/2001GL014018.

Pancheshnyi, S. (2000), Collisional deactivation of $N_2(C^3\Pi_u, v = 0, 1, 2, 3)$ states by N_2, O_2, H_2 and H_2O molecules, *Chem. Phys.*, *262*, 349–357, doi:10.1016/S0301-0104(00)00338-4.

Piper, L. G. (1988), State-to-state $N_2(A^3\Sigma_u^+)$ energy pooling reactions. II. The formation and quenching of $N_2(B^3\Pi_g, v = 1–12)$, *J. Chem. Phys.*, *88*, 6911–6921, doi:10.1063/1.454388.

Sentman, D. D., H. C. Stenbaek-Nielsen, M. G. McHarg, and J. S. Morrill (2008a), Correction to "Plasma chemistry of sprite streamers", *J. Geophys. Res.*, *113*, D14399, doi:10.1029/2008JD010634.

Sentman, D. D., H. C. Stenbaek-Nielsen, M. G. McHarg, and J. S. Morrill (2008b), Plasma chemistry of sprite streamers, *J. Geophys. Res.*, *113*, D11112, doi:10.1029/2007JD008941.

Siefring, C. L., J. S. Morrill, D. D. Sentman, and M. J. Heavner (2010), Simultaneous near-infrared and visible observations of sprites and acoustic gravity waves during the EXL98 campaign, *J. Geophys. Res.*, *115*, A00E57, doi:10.1029/2009JA014862.

Simek, M. (2002), The modelling of streamer-induced emission in atmospheric pressure, pulsed positive corona discharge: N_2 second positive and NO-γ systems, *J. Phys. D Appl. Phys.*, *35*, 1967, doi:10.1088/0022-3727/35/16/311.

Stenbaek-Nielsen, H. C., M. G. McHarg, T. Kanmae, and D. D. Sentman (2007), Observed emission rates in sprite streamer heads, *Geophys. Res. Lett.*, *34*, L11105, doi:10.1029/2007GL029881.

F. J. Gordillo-Vázquez and A. Luque, Instituto de Astrofísica de Andalucía, CSIC, PO Box 3004, E-18080 Granada, Spain. (vazquez@iaa.es; aluque@iaa.es)